RM A58D28

NACA RM A58D28

RESEARCH MEMORANDUM

TURBULENT SKIN FRICTION AT HIGH MACH NUMBERS AND REYNOLDS NUMBERS

By Fred W. Matting and Dean R. Chapman

Ames Aeronautical Laboratory
Moffett Field, Calif.

NATIONAL ADVISORY COMMITTEE
FOR AERONAUTICS
WASHINGTON

NACA RM A58D28

NATIONAL ADVISORY COMMITTEE FOR AERONAUTICS

RESEARCH MEMORANDUM

TURBULENT SKIN FRICTION AT HIGH MACH NUMBERS AND REYNOLDS NUMBERS

By Fred W. Matting and Dean R. Chapman

For a number of years now, experimenters have been making measurements of skin friction. Formerly, the main interest was at low Mach numbers; later, measurements were made at supersonic Mach numbers. However, almost all of these measurements were over a limited range of Reynolds numbers. On the other hand, these measurements fairly well determined the effects of Mach number and heat transfer on skin friction.

The purpose of this paper is to give the results of skin-friction measurements in turbulent boundary layers at high Mach numbers and high Reynolds numbers where data have not previously existed. The equipment used was expressly designed to provide these conditions. As is well known, it is difficult to obtain high Mach numbers and high Reynolds numbers simultaneously with air in a wind tunnel. In order to avoid condensation, it is necessary to heat the air, with a resulting loss in density and Reynolds number. It is desirable, then, to use a gas that does not condense at high Mach numbers. This suggested helium, which was used as a working fluid in some of the tests. At high Mach numbers in a given wind tunnel, higher Reynolds numbers can be obtained with helium than with air, principally because no heating of the helium is required. The different ratios of specific heats also contribute to the increase. In using helium as a working fluid, it is, of course, necessary to determine the equivalence of air and helium in the turbulent boundary layer.

Figure 1 is a sketch of the equipment used, the Ames 1- by 10-inch boundary-layer channel. The test section is 10 inches wide and has a nominal height of 1 inch; these proportions assure an essentially two-dimensional flow. Although this equipment is called a channel, studies were not made of channel flows. There was always a core of potential flow between the top and the bottom boundary layers. The nozzle block is adjustable, which allows the setting of different Mach numbers and pressure gradients. The scope of the present series of tests included only the zero pressure gradient case. Direct measurements of local skin friction were made by means of the skin-friction element shown. This element consists of a disc 2-1/4 inches in diameter suspended from flexures. The force on the disc is measured by means of a differential transformer. Corrections were made for buoyancy forces surrounding the disc; these were generally found to be negligible. An optical interferometer was used to assure that the disc was flush with its housing to within a half wavelength of light. Both the disc and the top plate have very smooth finishes, the disc being finished to 4 microinches and

the top plate to 15 microinches. Not shown in figure 1 is a heater which allows control of the stagnation temperature of the working fluid.

In the present tests, the stagnation temperature was set relative to the wall temperature, so that the boundary layers were adiabatic. The scope of the experiments to date, then, consists of direct measurements of local skin friction in turbulent boundary layers on a smooth flat plate at zero pressure gradient. The boundary layers were adiabatic. The speed in the tests was varied from low subsonic Mach numbers up to a Mach number of 6.7, while the Reynolds number range was from 1×10^6 to 120×10^6. At the highest Reynolds number the stagnation pressure was 700 pounds per square inch. In the calculations of Reynolds number the length used was from the center line of the element back to the virtual origin of turbulence as best it could be determined. Boundary-layer surveys were made at a number of upstream stations to determine the point of transition as a function of Mach number and Reynolds number for this tunnel. Over most of the range of Reynolds numbers it was found that the virtual origin was near the nozzle throat.

Figure 2 is a plot of Mach number against Reynolds number showing the test domain of the boundary-layer channel, which is everything to the left of the hatched line. For purposes of comparison, also shown is the so-called corridor of continuous flight, which is the approximate Mach number-Reynolds number regime for steady continuous level flight of airplane-like configurations. A characteristic length of 50 feet was used in the calculation. Most previous skin-friction data were taken in the area to the left and below the corridor of continuous flight. It is seen that the boundary-layer channel has extended the Mach number-Reynolds number range into a regime of considerable interest. (Even a further extension would be desirable.) It should also be noted that certain vehicles, such as ballistic missiles, actually operate outside (and above) the corridor of continuous flight. The shaded area at the bottom of the figure shows the regime in which tests have been conducted in the channel to date. Air was used as the working fluid up to a Mach number of 4.2, and helium from a Mach number of 4.2 up to a Mach number of 6.7.

On the question of the equivalence of air and helium in the turbulent boundary layer, a dimensional analysis of the differential equations of motion and energy for the turbulent boundary layer (at constant pressure) shows that in order to get dynamically similar boundary layers with two different gases, it is necessary to match the parameter $M\sqrt{\gamma-1}$, where $\gamma = C_p/C_v$. This parameter is also valid for the laminar boundary layer, but it should not be used for other types of flows. Figure 3 shows the equivalence relation used:

$$M_a = M_{He}\sqrt{\frac{\gamma_{He}-1}{\gamma_{AIR}-1}} \approx 1.29\, M_{He}$$

where M_a is the equivalent air Mach number for a helium flow at the actual Mach number M_{He}. Figure 3 shows a comparison of air and helium flows at actual Mach numbers of 4.20 and 3.25, respectively. Since both of these flows are at an equivalent air Mach number of 4.20, one would expect them to be dynamically similar in the turbulent boundary layer. The plot in figure 3 of the local skin-friction coefficient against Reynolds number shows that the air and helium points do fall on one curve. Also, by comparison with the curve for $M_a = 0$, it is noted that the sizable reduction of C_f (which is a measure of compressibility effects) is the same for the two gases. This is the experimental verification of the equivalence of air and helium in the turbulent boundary layer.

In addition to matching the Mach number parameter, it is also necessary to match the ratio of wall temperature to free-stream temperature for the two gases used. In the adiabatic case this is automatically accomplished by using the Mach number parameter (assuming equal recovery factors).

It was stated previously that at high Mach numbers in a given wind tunnel one can obtain higher Reynolds numbers with helium than with air. To illustrate this, in the Ames 1- by 10-inch boundary-layer channel at an equivalent air Mach number of 15, a Reynolds number of 25×10^6 can be expected if helium is used. To obtain this same Reynolds number with air would require a test section 150 feet long and the air would have to be heated to $4{,}600^\circ$ R; in other words, at this Mach number the Reynolds number factor is about 75 to 1.

Figure 4 largely summarizes the data taken to date. It is a plot of the local skin-friction coefficient against Reynolds number, at equivalent air Mach numbers ranging from 0.2 to 6.70. It is noted that the subsonic data agree well with that taken by other experimenters. The broken line represents data taken in the Ames 12-foot pressure tunnel (ref. 1), while the dotted line is the Kármán-Schoenherr incompressible curve. The importance of the subsonic data lies in the fact that it shows no roughness effects or roughness "bend-up." When appreciable roughness exists, the subsonic skin-friction curve should, with increasing Reynolds number, diverge upward from the curve for a smooth surface and eventually become horizontal. No such effects are seen here. This is noted because it is seen that there is a slight bend-up in the supersonic curves at the highest Reynolds numbers. It is believed that this trend is not due to roughness since all the data were taken on the same plate and with the same skin-friction element. A number of investigators have shown that high Mach number boundary layers are less sensitive to roughness than are subsonic boundary layers. (This is probably due to the high Mach number boundary layers having thicker laminar sublayers.) Therefore, since no roughness effects in the subsonic measurements are to be seen, it is felt that the supersonic measurements are also free from roughness effects.

Figure 5 is a plot of the ratio of the local skin-friction coefficient to the incompressible local skin-friction coefficient at the same Reynolds number (C_f/C_{f_i}) plotted against Reynolds number. The dashed lines represent calculated values of C_f/C_{f_i} calculated by the T' or intermediate enthalpy method. This method uses a mean reference temperature to evaluate the physical properties of the gas. The method was originally used by Rubesin and Johnson (ref. 2) for laminar flows and was adapted to turbulent flows by Eckert, Sommer, and Short, and others. The constants used in the calculations are those determined by Sommer and Short (ref. 3). (Constants obtained by other investigators do not change the results much.) It is seen that the experimental data and the T' calculations agree quite well; however, the trends are slightly different with Reynolds number. To date, no satisfactory explanation of the bend-up in C_f/C_{f_i} at the highest Reynolds numbers has been found. However, this effect is actually small, as is seen in figure 4. The large effect on C_f is due to Mach number, as shown in figure 4. (There is another large effect due to heat-transfer conditions, but this was not in the scope of the present investigation.) It has been known for some time that the T' method gives good predictions for the effects on skin friction of Mach number and heat transfer at moderate Reynolds numbers. It is now seen that the T' method gives good answers over a surprisingly large Reynolds number range. This is probably the most important result of this paper.

It should be emphasized again that these data were taken in adiabatic boundary layers. To calculate C_f in a nonadiabatic boundary layer, one could start with C_{f_i}, say the Kármán-Schoenherr value, and then use the T' method. This method gives good predictions for the effects of Mach number and heat transfer on C_f, and, as has been shown, the T' method also gives a fairly good prediction for the effect of Reynolds number on skin friction.

Ames Aeronautical Laboratory
National Advisory Committee for Aeronautics
Moffett Field, Calif., Mar. 20, 1958

REFERENCES

1. Smith, Donald W., and Walker, John H.: Skin-Friction Measurements in Incompressible Flow. NACA TN 4231, 1958.

2. Rubesin, M. W., and Johnson, H. A.: A Critical Review of Skin-Friction and Heat-Transfer Solutions of the Laminar Boundary Layer of a Flat Plate. Trans. A.S.M.E., vol. 71, no. 4, May 1949.

3. Sommer, Simon C., and Short, Barbara J.: Free-Flight Measurements of Turbulent-Boundary-Layer Skin Friction in the Presence of Severe Aerodynamic Heating at Mach Numbers From 2.8 to 7.0. NACA TN 3391, 1955.

1-BY 10-INCH BOUNDARY-LAYER CHANNEL

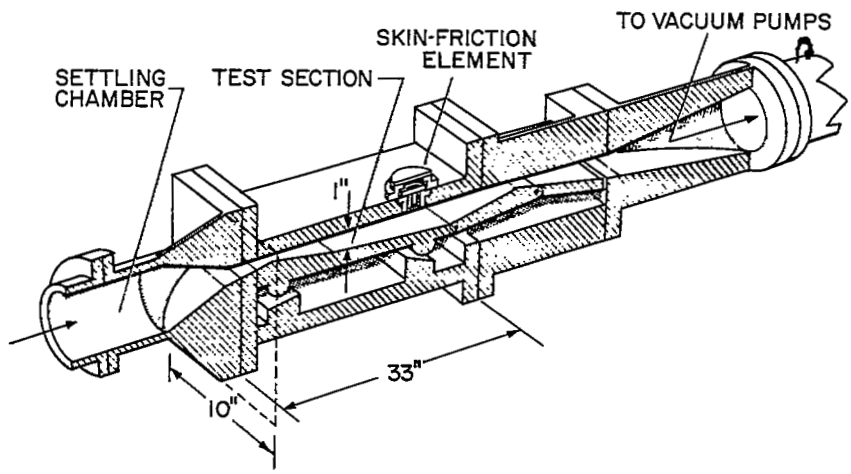

Figure 1

TEST DOMAIN

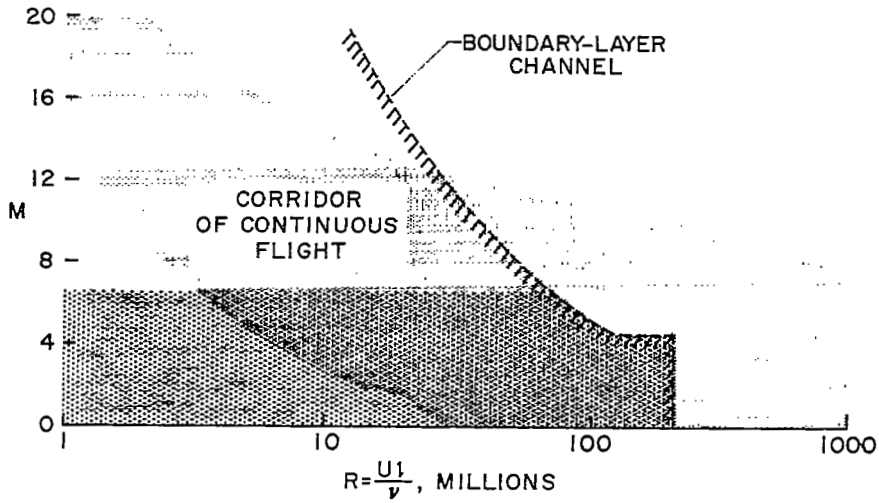

Figure 2

EQUIVALENCE OF AIR AND HELIUM
TURBULENT SKIN FRICTION

$$\text{EQUIVALENT AIR MACH NO.} = M_a \equiv M_{He}\sqrt{\frac{\gamma_{He}-1}{\gamma_{AIR}-1}} \approx 1.29\,M_{He}$$

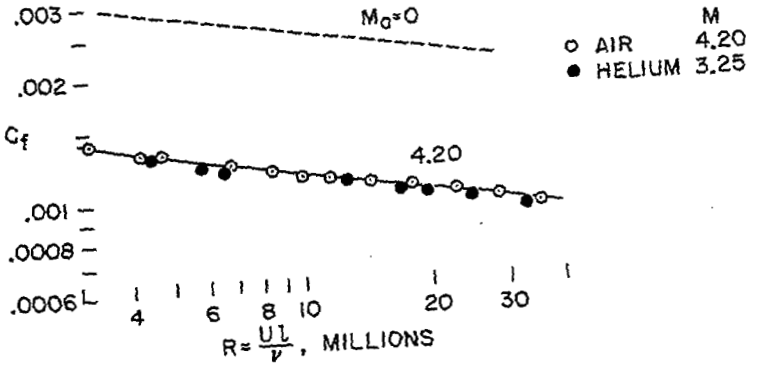

Figure 3

FLAT PLATE TURBULENT SKIN FRICTION

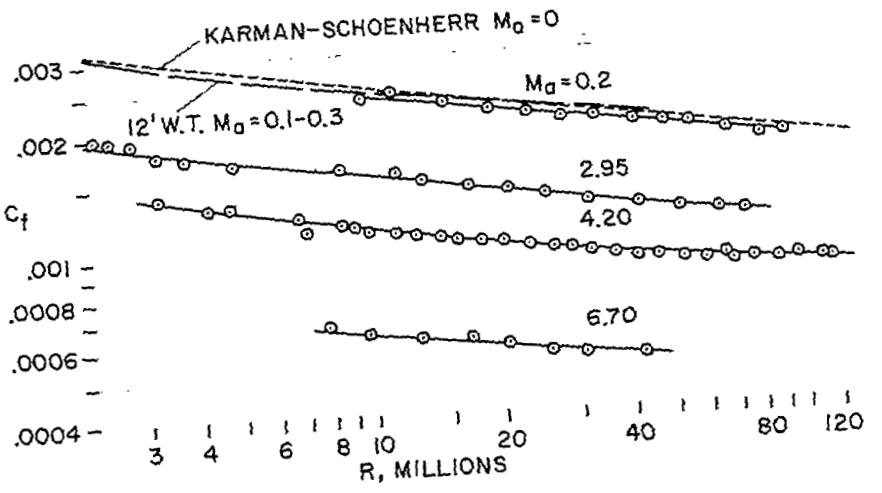

Figure 4

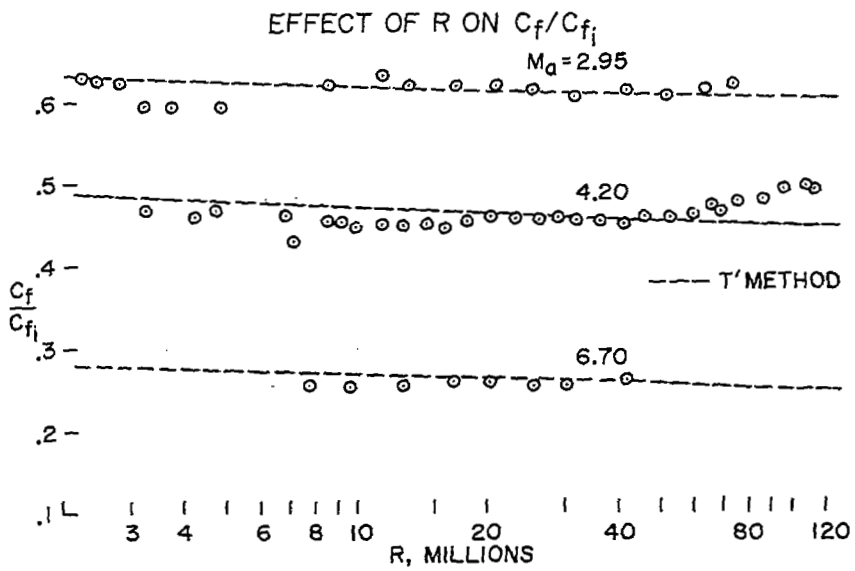
EFFECT OF R ON C_f/C_{f_i}
M_a = 2.95
4.20
6.70
T' METHOD
$\frac{C_f}{C_{f_i}}$
.6
.5
.4
.3
.2
.1
3
4
6
8
10
20
40
80
120
R, MILLIONS

Figure 5